UPPSALA
UNIVERSITET

Digital Comprehensive Summaries of Uppsala Dissertations from the Faculty of Science and Technology 1463

Efficient Simulation of Wave Phenomena

MARTIN ALMQUIST

ACTA
UNIVERSITATIS
UPSALIENSIS
UPPSALA
2017

ISSN 1651-6214
ISBN 978-91-554-9777-4
urn:nbn:se:uu:diva-310124

Dissertation presented at Uppsala University to be publicly examined in Room 2446, ITC, Lägerhyddsvägen 2, Uppsala, Friday, 10 February 2017 at 10:15 for the degree of Doctor of Philosophy. The examination will be conducted in English. Faculty examiner: Associate Professor Gianluca Iaccarino (Center for Turbulence Research, Department of Mechanical Engineering, Stanford University).

Abstract
Almquist, M. 2017. Efficient Simulation of Wave Phenomena. *Digital Comprehensive Summaries of Uppsala Dissertations from the Faculty of Science and Technology* 1463. 42 pp. Uppsala: Acta Universitatis Upsaliensis. ISBN 978-91-554-9777-4.

Wave phenomena appear in many fields of science such as acoustics, geophysics, and quantum mechanics. They can often be described by partial differential equations (PDEs). As PDEs typically are too difficult to solve by hand, the only option is to compute approximate solutions by implementing numerical methods on computers. Ideally, the numerical methods should produce accurate solutions at low computational cost. For wave propagation problems, high-order finite difference methods are known to be computationally cheap, but historically it has been difficult to construct stable methods. Thus, they have not been guaranteed to produce reasonable results.

In this thesis we consider finite difference methods on summation-by-parts (SBP) form. To impose boundary and interface conditions we use the simultaneous approximation term (SAT) method. The SBP-SAT technique is designed such that the numerical solution mimics the energy estimates satisfied by the true solution. Hence, SBP-SAT schemes are energy-stable by construction and guaranteed to converge to the true solution of well-posed linear PDE. The SBP-SAT framework provides a means to derive high-order methods without jeopardizing stability. Thus, they overcome most of the drawbacks historically associated with finite difference methods.

This thesis consists of three parts. The first part is devoted to improving existing SBP-SAT methods. In Papers I and II, we derive schemes with improved accuracy compared to standard schemes. In Paper III, we present an embedded boundary method that makes it easier to cope with complex geometries. The second part of the thesis shows how to apply the SBP-SAT method to wave propagation problems in acoustics (Paper IV) and quantum mechanics (Papers V and VI). The third part of the thesis, consisting of Paper VII, presents an efficient, fully explicit time-integration scheme well suited for locally refined meshes.

Keywords: finite difference method, high-order accuracy, stability, summation by parts, simultaneous approximation term, quantum mechanics, Dirac equation, local time-stepping

Martin Almquist, Department of Information Technology, Division of Scientific Computing, Box 337, Uppsala University, SE-751 05 Uppsala, Sweden.

ISSN 1651-6214
ISBN 978-91-554-9777-4
urn:nbn:se:uu:diva-310124 (http://urn.kb.se/resolve?urn=urn:nbn:se:uu:diva-310124)

List of papers

This thesis is based on the following papers, which are referred to in the text by their Roman numerals.

I K. Mattsson and M. Almquist. A solution to the stability issues with block norm summation by parts operators. *Journal of Computational Physics*, 253:418-442, 2013.

II K. Mattsson, M. Almquist and M. H. Carpenter. Optimal diagonal-norm SBP operators. *Journal of Computational Physics* 264:91-111, 2014.

III K. Mattsson and M. Almquist. A high-order accurate embedded boundary method for first order hyperbolic equations. *Accepted for publication in Journal of Computational Physics*, 2016.

IV M. Almquist, I. Karasalo, and K. Mattsson. Atmospheric Sound Propagation Over Large-Scale Irregular Terrain. *Journal of Scientific Computing* 61:369-397, 2014.

V M. Almquist, K. Mattsson and T. Edvinsson. High-fidelity numerical solution of the time-dependent Dirac equation. *Journal of Computational Physics*, 262:86-103, 2014.

VI E. Sjöqvist, M. Almquist, K. Mattsson, Z. N. Gürkan, and B. Hessmo. Realization of adiabatic Aharonov-Bohm scattering with neutrons. *Physical Review A*, 92:52108, 2015.

VII M. Almquist and M. Mehlin. Multi-level Runge–Kutta based local time-stepping methods for wave propagation. *Preprint, Department of Information Technology, Uppsala University*, 2016. (Submitted)

Reprints were made with permission from the publishers.

Contents

1. Introduction

Waves appear in many shapes in the world we live in: the sounds we hear are pressure waves, the tremors we sense during an earthquake are seismic waves, and the water waves we can see on a lake are gravity waves. Less obvious to our senses, yet fundamentally important, are quantum mechanical waves—on atomistic length scales, subatomic particles may behave as waves and waves may behave as massive particles. Visible light, for instance, clearly exhibits wave-like behavior as it is dispersed by water droplets to form a rainbow. Yet the photoelectric effect, whereby a metal exposed to light of sufficiently short wavelength will emit electrons, can only be satisfactorily explained if light beams consist of discrete packets or particles (known as photons) rather than waves. Similarly, electrons, protons, and neutrons, although often thought of as massive particles, frequently exhibit wave-like behavior.

The wave phenomena mentioned above have in common that they are governed by partial differential equations (PDEs). The advection equation in one dimension provides the simplest example of a PDE describing wave propagation,

$$\begin{aligned} &u_t + u_x = 0\,, \quad x \in (0,L)\,, \quad t > 0\,, \\ &u(0,t) = g(t)\,, \qquad\qquad\quad t > 0\,, \end{aligned} \tag{1.1}$$

where subscripts denote partial derivatives, x is the spatial coordinate, t the time variable, and $g(t)$ a known function. We assume that the solution u is known at the initial time $t = 0$. The equation (1.1) propagates features in $u(x,t)$ to the right with unit speed. At the outlet $x = L$, the features simply leave the domain. At the inlet $x = 0$ however, we must specify what is flowing into the domain—this is accomplished by the boundary condition $u(0,t) = g(t)$. Without the boundary condition, the solution would not be unique.

While (1.1) is simple enough that it can be solved on the back of an envelope, PDEs are more often than not so complex that we have to resort to numerical approximation algorithms to solve them. As the title suggests, this text concerns *efficient* numerical methods. To explain what makes an efficient method, we consider the numerical solution of (1.1). There are many numerical methods for PDE, but they all involve representing the solution u by a finite number of values. For example, one may discretize the spatial part of (1.1) by introducing the equidistant grid points

$$x_j = (j-1)h, \quad j = 1,\ldots,N\,, \tag{1.2}$$

where $h = \frac{L}{N-1}$. We may then introduce a discrete solution vector $\mathbf{u} = [u_1, u_2, \ldots, u_N]^T$, where $u_i(t)$ is intended to approximate $u(x_i, t)$. Approximating the spatial derivative by for example finite differences leads to a system of N ordinary differential equations (ODEs),

$$\frac{\mathrm{d}\mathbf{u}}{\mathrm{d}t} = M\mathbf{u} + \mathbf{G}(t), \tag{1.3}$$

where the exact forms of the matrix M and the vector-valued function $\mathbf{G}(t)$ depend on the method used. The equation is a semi-discrete problem in the sense that we have discretized space while leaving time continuous. Solving (1.1) of course requires discretizing the time variable too, but for now we focus on the spatial discretization.

By applying a numerical method to (1.1), we have transitioned from a single PDE to a system of ODEs. This is good because ODEs are conceptually simpler than PDEs, but also bad because we now face a system of N equations (the reader should think of N as large). Solving (1.3) will inevitably require many arithmetic operations, which makes it a daunting task for a human being. Computers, however, are very good at arithmetic. Modern computers can easily perform billions of operations per second. By implementing numerical algorithms on computers, it is possible to simulate many kinds of wave phenomena governed by PDEs far more complicated than (1.1).

At this point, a word of caution is called for. Even for the simple equation (1.1), naïve numerical methods may fail spectacularly—for instance, unstable methods will cause the numerical solution to grow exponentially in time even though the true solution does not grow. To avoid such setbacks, we call for *robust* numerical methods, which produce reasonable results in many different settings. An ideal method should be guaranteed to converge to the true solution as N increases (or, equivalently, as h decreases). Of course, the drawback to increasing N is that the algorithm becomes more computationally demanding, which means that the simulation will take longer to run. Hence, to be able to solve large problems, it is imperative to use *cheap* numerical methods. By cheap we here mean that, when all goes well, the method requires few computational resources to compute the solution to within a specified error tolerance.

In addition to computational resources, we should consider the manpower spent on implementing numerical algorithms. Naturally, a desirable property is that the method is *simple* in the sense that it is easy to program, but that is not all. When investigating wave phenomena, the exact form of the equations of interest is typically not known a priori. More often than not, one wants to investigate what happens when certain parameters are changed slightly. If the numerical method is too tightly tied to a certain problem, we may be forced to switch to a different method, which results in a lot of extra work. We therefore seek *flexible* methods, which with only minor modifications can treat wide

ranges of parameters in the equations, different types of boundary conditions, and so on.

Based on the considerations above, we conclude that efficient numerical methods should be robust, cheap, simple, and flexible. For numerical solution of PDEs there are many methods available, all of which have their strengths and weaknesses. Popular methods include finite volume, finite element, finite difference and spectral methods. In this thesis we will work with finite difference methods. They are conceptually simple as well as easy to implement in an efficient manner. For wave propagation problems, high-order methods are typically cheaper than low-order methods [27]. Compared to finite volume and finite element methods, finite difference methods are advantageous because they can be extended to high order while naturally allowing for fully explicit time-stepping. Unfortunately, increasing the order of accuracy tends to make difference methods less robust when non-periodic boundary conditions are considered. Hence, practitioners were often forced to trade cheapness for robustness in the past. Today, so-called summation-by-parts–simultaneous-approximation-term finite difference methods [10, 39] have resolved this dilemma by providing a means to systematically construct robust high-order methods. The technique is flexible in the sense that it applies to a wide variety of PDEs and boundary conditions.

We will give an introduction to the summation-by-parts technique in Chapter 3. We proceed to consider multi-dimensional settings in Chapter 4 and complex geometries in Chapter 5. But before discussing numerical techniques, we take a closer look at the wave equations governing quantum mechanics in Chapter 2.

2. Quantum mechanical waves

On the scale of atoms, classical physics fails to describe nature. The scientific field that explains the microscopic world of subatomic particles is known as quantum mechanics. Because human intuition is based on our observations of the macroscopic world, many features of quantum mechanics may seem counter-intuitive. A quantum mechanical system is completely described by its wave function, which provides probability densities for measurable quantities such as position and momentum. Measurements of the position of a particle in a single-particle system may be regarded as realizations of a stochastic variable with the probability density function corresponding to the system's wave function.

The evolution of the wave function is usually described by the time-dependent Schrödinger equation (SE) [35], which is a scalar PDE. For a single-particle system, the PDE can be posed on the regular physical three-dimensional space. For a quantum system with N_p particles, however, the wave function describing the system lives in an abstract $3N_p$-dimensional space. If one is not interested in the absolute position and orientation of the system, which is typically the case, the number of dimensions can be reduced to $3N_p - 6$. Still, quantum mechanical equations are often very high-dimensional.

The SE is not consistent with the theory of relativity. Hence, it does not provide an accurate description for high-energy systems, where particle velocities approach the speed of light. A better model for such cases is the Dirac equation (DE) [12], in which the wave function is a vector of four components. For a quantum system consisting of a single electron, the wave function can be regarded as a superposition of a spin-up electron, a spin-down electron, a spin-up positron, and a spin-down positron. Thus, in addition to incorporating relativity, the DE describes spin evolution as well as particle-antiparticle interactions.

The remaining part of this chapter is devoted to analyzing and comparing the SE and DE from a mathematical point of view.

2.1 The Schrödinger equation

The SE for a single particle in an electric field reads

$$i\hbar\psi_t = \left(-\frac{\hbar^2}{2m}\Delta + qU\right)\psi,$$

where $\psi = \psi(\mathbf{r},t)$ is the wave function, $\mathbf{r}$ denotes position, m is the particle's mass, q its charge, $\hbar$ the reduced Planck constant, and U the electric potential. In free space (that is, when $U = 0$), the equation admits plane-wave solutions

$$\psi(\mathbf{r},t) = e^{\frac{i}{\hbar}(\mathbf{r}\cdot\mathbf{p}-Et)},$$

where E is the classical kinetic energy corresponding to momentum $p = |\mathbf{p}|$,

$$E = \frac{p^2}{2m}.$$

We note that the spatial frequency (or wavenumber) of a wave is proportional to the momentum, while the temporal frequency is proportional to the energy. The group velocity is

$$c_g = \frac{\partial E}{\partial p} = \frac{p}{m},$$

which shows that the SE is dispersive—the group velocity grows linearly with the wavenumber. The unbounded wave speed makes the SE difficult to solve numerically, partly because of stringent constraints on the time-step for explicit time-integrators.

2.2 The Dirac equation

The DE for a spin-$\frac{1}{2}$ particle in an electrostatic potential reads

$$i\hbar\psi_t = H\psi, \tag{2.1}$$

where the Hamiltonian operator H is given by

$$H\psi = (c\vec{\alpha}\cdot\hat{\mathbf{p}} + mc^2\beta + qU)\psi. \tag{2.2}$$

The first term in the right-hand side of (2.2) is related to kinetic energy; c denotes the speed of light and $\hat{\mathbf{p}} = -i\hbar\nabla$ is the momentum operator. The second term is the rest energy; m denotes particle mass. The third term corresponds to potential energy; q is the electric charge of the particle and U is the electric potential.

The operators $\vec{\alpha}$ and β are defined as

$$\vec{\alpha} = (\alpha_1,\alpha_2,\alpha_3), \quad \beta = \begin{bmatrix} I_2 & 0 \\ 0 & -I_2 \end{bmatrix},$$

where I_2 denotes the 2-by-2 identity matrix and the α_i can be expressed in terms of the Pauli matrices σ_i as

$$\alpha_i = \begin{bmatrix} 0 & \sigma_i \\ \sigma_i & 0 \end{bmatrix}, \quad i = 1,2,3.$$

The Pauli matrices are

$$\sigma_1 = \begin{bmatrix} 0 & 1 \\ 1 & 0 \end{bmatrix}, \quad \sigma_2 = \begin{bmatrix} 0 & -i \\ i & 0 \end{bmatrix}, \quad \sigma_3 = \begin{bmatrix} 1 & 0 \\ 0 & -1 \end{bmatrix}.$$

The DE is a hyperbolic system of four equations. For a particle in free space the electric potential is zero and (2.1) admits analytic plane-wave solutions of the form

$$\psi(\mathbf{r},t) = \mathbf{u}_\mathbf{p} e^{\frac{i}{\hbar}(\mathbf{r}\cdot\mathbf{p} - E_p t)},$$

where the momentum vector is $\mathbf{p} = (p_x, p_y, p_z)$ and the relativistic energy corresponding to momentum $p = |\mathbf{p}|$ is

$$E_p^2 = p^2c^2 + m^2c^4. \tag{2.3}$$

For positive energies $E_p = \sqrt{p^2c^2 + m^2c^4}$ there are two linearly independent solutions:

$$\mathbf{u}_\mathbf{p}^{(1)} = \begin{bmatrix} 1 \\ 0 \\ \frac{cp_z}{E_p + mc^2} \\ \frac{c(p_x + ip_y)}{E_p + mc^2} \end{bmatrix} \quad \text{and} \quad \mathbf{u}_\mathbf{p}^{(2)} = \begin{bmatrix} 0 \\ 1 \\ \frac{c(p_x - ip_y)}{E_p + mc^2} \\ \frac{-cp_z}{E_p + mc^2} \end{bmatrix}.$$

For negative energies $E_p = -\sqrt{p^2c^2 + m^2c^4}$ we have

$$\mathbf{u}_\mathbf{p}^{(3)} = \begin{bmatrix} \frac{-cp_z}{|E_p| + mc^2} \\ \frac{-c(p_x + ip_y)}{|E_p| + mc^2} \\ 1 \\ 0 \end{bmatrix} \quad \text{and} \quad \mathbf{u}_\mathbf{p}^{(4)} = \begin{bmatrix} \frac{-c(p_x - ip_y)}{|E_p| + mc^2} \\ \frac{cp_z}{|E_p| + mc^2} \\ 0 \\ 1 \end{bmatrix}.$$

Without restriction we now let the momentum be directed along the positive x-direction such that $p = p_x$ and $p_y = p_z = 0$, which yields

$$\psi(\mathbf{r},t) = \mathbf{u}_\mathbf{p} e^{\frac{i}{\hbar}(px - E_p t)}.$$

Differentiating (2.3) with respect to p yields

$$2E_p \frac{\partial E_p}{\partial p} = 2pc^2.$$

Hence, the group velocity is

$$c_g = \frac{\partial E_p}{\partial p} = \frac{pc^2}{E_p}.$$

In the classical limit of low kinetic energy, we have $p << mc$ such that for $E_p > 0$ we get

$$c_g = \frac{pc^2}{\sqrt{p^2c^2 + m^2c^4}} = \frac{pc}{\sqrt{p^2 + (mc)^2}} \approx \frac{pc}{\sqrt{(mc)^2}} = \frac{p}{m}.$$

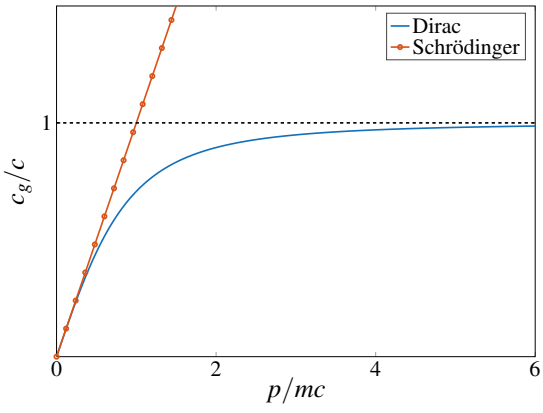

Figure 2.1. Group velocity as a function of momentum for the Schrödinger and Dirac equations.

This shows that, in the classical limit, the dispersion relation is exactly the same as that of the SE; large wavenumbers (or large momenta) travel faster than small ones. In the relativistic limit $p >> mc$, however, we obtain

$$c_g = \frac{pc^2}{\sqrt{p^2c^2 + m^2c^4}} = \frac{pc}{\sqrt{p^2 + (mc)^2}} \approx \frac{pc}{\sqrt{p^2}} = c\,.$$

Thus, as the momentum tends to infinity, the group velocity approaches—but does not exceed—the speed of light. This is consistent with the theory of special relativity, which states that no information can propagate faster than the speed of light. Since the SE does not incorporate relativity, it violates this principle. The group velocities as functions of momentum are presented in Figure 2.1. An interesting observation is that the unlimited wave speed, which is part of the difficulty associated with numerical solution of the SE, is to some extent an artefact of an incomplete model.

3. The summation-by-parts finite difference method

Wave propagation problems often feature waves that are transported long distances. In such settings, the ground-breaking 1972 paper [27] by Kreiss and Oliger showed that high-order finite difference methods outperform second-order methods by requiring far fewer degrees of freedom for a given error tolerance. After that, there was a surge of interest in high-order difference methods. While it is easy to construct stable high-order schemes for periodic problems, it is non-trivial to find accurate and stable schemes close to boundaries. Kreiss and Scherer [26, 34] took the first step towards stable difference schemes by developing the summation-by-parts (SBP) concept. In 1994, Carpenter et al. [6] combined SBP operators with the simultaneous approximation term (SAT) method of imposing boundary and interface conditions weakly. The combined SBP-SAT method leads to semi-discrete approximations that satisfy energy estimates completely analogous to the energy estimates of the true solution. Thus, the method allows for stability proofs via the energy method.

3.1 The continuous problem

To introduce the SBP-SAT method, we again consider the advection equation (1.1). Let $v, w \in L^2[0,L]$ be smooth complex-valued functions and let $(\cdot,\cdot)$ and $\|\cdot\|$ denote the standard L^2 inner product and norm such that

$$(v,w) = \int_0^L v^* w \,\mathrm{d}x\,, \quad \|v\|^2 = (v,v),$$

where * denotes conjugate transpose. For future use we note that the integration-by-parts formula can be expressed in terms of the inner product as

$$(v,w_x) = v^* w|_0^L - (v_x,w)\,. \tag{3.1}$$

In the special case $v = w$, the formula (3.1) reduces to

$$(v,v_x) + (v_x,v) = |v|^2\big|_0^L\,. \tag{3.2}$$

Now, we shall attempt to estimate how fast the solution u of (1.1) grows in time. To this end, we use what is called the energy method. That is, we multiply the PDE by u^* and integrate in space, which yields

$$(u, u_t) = -(u, u_x)\,. \tag{3.3}$$

Adding (3.3) and its conjugate transpose leads to

$$(u, u_t) + (u_t, u) = -(u, u_x) - (u_x, u) = -\left|u\right|^2\Big|_0^L\,,$$

where we used the formula (3.2). By noting that $(u, u_t) + (u_t, u) = \frac{\mathrm{d}}{\mathrm{d}t}\|u\|^2$ and using the boundary condition, we obtain the energy estimate

$$\frac{\mathrm{d}}{\mathrm{d}t}\|u(\cdot,t)\|^2 = |g(t)|^2 - |u(L,t)|^2\,.$$

With the homogeneous boundary condition, that is when $g = 0$, we find that

$$\frac{\mathrm{d}}{\mathrm{d}t}\|u(\cdot,t)\|^2 = -\left|u(L,t)\right|^2 \leq 0\,, \tag{3.4}$$

which shows that $\|u(\cdot,t)\|$ is non-increasing in time.

3.2 The semi-discrete problem

We now seek a convergent finite difference scheme. By the famous theorem due to Lax and Richtmyer [28], for well-posed linear PDE the approximate solution converges to the true solution if and only if the method is stable and consistent. Since all reasonable methods are consistent by construction, stability and convergence will be equivalent in our discussion. Loosely speaking, a scheme is stable if the approximate solution does not grow uncontrollably. If we can derive an energy estimate for the semi-discrete solution similar to the continuous energy estimate (3.4), which shows that the solution is non-increasing, then that is certainly enough for stability (in principle the semi-discrete solution could be allowed to grow in time [19]).

We introduce the N equidistant grid points in (1.2). Let $\mathbf{u}(t) \in \mathbb{C}^N$ denote the semi-discrete solution vector, $\mathbf{u} = [u_1, u_2, \ldots, u_N]^T$. A Hermitian positive definite matrix $P \in \mathbb{C}^{N\times N}$ induces an inner product $(\mathbf{v}, \mathbf{w})_P = \mathbf{v}^* P \mathbf{w}$ with corresponding norm $\|\mathbf{v}\|_P^2 = (\mathbf{v}, \mathbf{v})_P$, for $\mathbf{v}$, $\mathbf{w} \in \mathbb{C}^N$. We also introduce the vectors

$$\mathbf{e}_l = [1, 0, \ldots, 0]^T\,, \quad \mathbf{e}_r = [0, \ldots, 0, 1]^T\,,$$

such that $\mathbf{e}_l^T \mathbf{u} = u_1$ and $\mathbf{e}_r^T \mathbf{u} = u_N$.

To derive an energy estimate for the discrete solution, we will need a special approximation of the spatial derivative:

Definition 1. A matrix D_1 is an SBP operator for the first derivative if it can be decomposed as

$$D_1 = H^{-1}\left(Q + \frac{1}{2}B\right),$$

where $H = H^T > 0$, $Q + Q^T = 0$, and $B = \mathbf{e}_r\mathbf{e}_r^T - \mathbf{e}_l\mathbf{e}_l^T = \begin{bmatrix} -1 & & \\ & & \\ & & 1 \end{bmatrix}$.

The matrix H will be referred to as the norm matrix. As we will see later, H must correspond to a quadrature rule. Thus, if $\mathbf{v}$ and $\mathbf{w}$ denote the restrictions of the functions v and w to the grid, then $(\mathbf{v},\mathbf{w})_H$ approximates (v,w). The rationale for Definition 1 is that D_1 mimics the integration-by-parts formula for the first derivative in the inner product defined by H. That is,

$$\begin{aligned}(\mathbf{v}, D_1\mathbf{w})_H &= \mathbf{v}^* H D_1 \mathbf{w} = \mathbf{v}^*\left(Q + \frac{1}{2}B\right)\mathbf{w} = \mathbf{v}^*\left(B - \frac{1}{2}B - Q^T\right)\mathbf{w} \\ &= \mathbf{v}^*\left(B - D_1^T H\right)\mathbf{w} = v_N^* w_N - v_1^* w_1 - (D_1\mathbf{v},\mathbf{w})_H,\end{aligned} \tag{3.5}$$

which is analogous to the continuous formula (3.1). In the special case $\mathbf{w} = \mathbf{v}$, the formula (3.5) simplifies to

$$(\mathbf{v}, D_1\mathbf{v})_H + (D_1\mathbf{v},\mathbf{v})_H = |v_N|^2 - |v_1|^2, \tag{3.6}$$

which mimics (3.2). Thus, the SBP operator allows us to construct a semi-discrete scheme such that the numerical solution mimics the true solution exactly when it comes to integrating by parts. Considering that the energy estimate (3.4) followed from the integration-by-parts formula, we may hope to derive a similar estimate for the semi-discrete solution. Using D_1 to discretize (1.1) in space leads to

$$\frac{\mathrm{d}\mathbf{u}}{\mathrm{d}t} + D_1\mathbf{u} = \tau(\mathbf{e}_l^T\mathbf{u} - g), \tag{3.7}$$

where we have added the SAT, which imposes the boundary condition, to the right-hand side. The SAT penalizes the solution by its deviation from the boundary condition, which makes the solution satisfy the boundary condition to the order of accuracy. The penalty parameter τ will be chosen such that the scheme is stable. By Duhamel's principle, it is enough to show stability for the homogeneous boundary condition [18], obtained when $g = 0$. Hence, we let $g = 0$ from now on. The discrete energy method, which amounts to multiplying (3.7) by $\mathbf{u}^* H$ from the left, yields

$$\left(\mathbf{u}, \frac{\mathrm{d}\mathbf{u}}{\mathrm{d}t}\right)_H = -(\mathbf{u}, D_1\mathbf{u})_H + \mathbf{u}^* H\tau(\mathbf{e}_l^T\mathbf{u} - 0).$$

The Ansatz $\tau = \sigma H^{-1}\mathbf{e}_l$, where σ is a real scalar, yields

$$\left(\mathbf{u}, \frac{\mathrm{d}\mathbf{u}}{\mathrm{d}t}\right)_H = -(\mathbf{u}, D_1\mathbf{u})_H + \sigma \mathbf{u}^* \mathbf{e}_l (\mathbf{e}_l^T \mathbf{u} - 0) = -(\mathbf{u}, D_1\mathbf{u})_H + \sigma |u_1|^2 . \quad (3.8)$$

Adding (3.8) and its conjugate transpose leads to

$$\left(\mathbf{u}, \frac{\mathrm{d}\mathbf{u}}{\mathrm{d}t}\right)_H + \left(\frac{\mathrm{d}\mathbf{u}}{\mathrm{d}t}, \mathbf{u}\right)_H = -(\mathbf{u}, D_1\mathbf{u})_H - (D_1\mathbf{u}, \mathbf{u})_H + 2\sigma |u_1|^2 .$$

By (3.6), we get

$$\frac{\mathrm{d}}{\mathrm{d}t}\|\mathbf{u}\|_H^2 = -|u_N|^2 + |u_1|^2 + 2\sigma |u_1|^2 = -|u_N|^2 + (1+2\sigma)|u_1|^2 .$$

We obtain an energy estimate if $1 + 2\sigma \leq 0$ so that

$$\frac{\mathrm{d}}{\mathrm{d}t}\|\mathbf{u}\|_H^2 = -|u_N|^2 + (1+2\sigma)|u_1|^2 \leq -|u_N|^2 \leq 0 ,$$

which shows that also $\|\mathbf{u}\|_H$ is non-increasing in time. That is, the scheme is stable.

Although any $\sigma \leq -1/2$ is sufficient for stability, the choice $\sigma = -1$ is often optimal. It makes the scheme dual-consistent, which leads to super convergence for linear functionals of the solution [5, 20]. A very large $|\sigma|$ would increase the spectral radius of the discretization and thus affect the time-step restriction negatively for explicit time-integrators.

We will show how to generalize the SBP-SAT method to multi-dimensional problems in Chapter 4. The technique also generalizes to systems of equations such as the Dirac equation, see for example Paper V. Furthermore, the SBP concept can be extended to order q derivatives by constructing discrete operators that mimic the integration-by-parts formula for inner products of the form $\left(v, \frac{\partial^q w}{\partial x^q}\right)$. D_1 applied q times is an SBP operator for the q:th derivative, but it is neither optimally cheap nor optimally accurate. In [29] and [30], Mattsson derived better operators for the second derivative with variable coefficients and constant-coefficient third and fourth derivatives.

3.3 The accuracy of SBP operators

We have shown that SBP operators enable us to construct provably stable schemes, but what is the accuracy of such schemes? We will use the following definition of accuracy:

Definition 2. Let $\mathbf{x}^q$ denote the restriction of the monomial $\frac{x^q}{q!}$ to the grid, with the convention that $\mathbf{x}^{-1} = \mathbf{0}$. We say that a difference operator D_1 for the first derivative is accurate of order p if the error

$$D_1\mathbf{x}^q - \mathbf{x}^{q-1}$$

vanishes for $q = 0, \ldots, p$.

The following result shows that for D_1 to be accurate, the norm matrix H must be an integrator.

Theorem 1. *A necessary condition for an SBP operator of order p to exist is that the entries in H be the weights of a quadrature rule of degree at least $p-1$.*

Proof. See e.g. [9]. □

In principle the SBP concept is very general; the SBP operator D_1 could be a full matrix and the grid need not be equidistant. Hence, many methods can be written on SBP form, including spectral collocation methods [7] and some discontinuous Galerkin and finite volume methods [15, 37]. In this thesis we consider finite difference methods exclusively. We will restrict ourselves to grids that are equidistant in the interior and only consider operators with a repeating stencil in the interior. The interior stencil will be a centered finite difference stencil of order $2p$, $p \in \mathbb{N}$, with minimal width. Close to the boundaries, we will have to transition from the centered stencil to skewed stencils in a way that retains the SBP properties in Definition 1. It turns out that the boundary stencils will necessarily be less accurate than the interior stencil; how much less depends on the requirements we place on the norm matrix H. We will discuss the accuracy of diagonal norm and block-diagonal norm SBP operators later in this section. First, we discuss how the locally reduced accuracy affects the global convergence rate.

3.3.1 Convergence rates for difference approximations

Gustafsson and Abarbanel et al. [1, 17] showed that, under certain assumptions, difference schemes with interior accuracy p_i and reduced accuracy p_b at a fixed number of points close to the boundaries converge with order $p_b + 1$ for first order hyperbolic equations. The assumptions are usually satisfied by SBP-SAT discretizations of interior accuracy two, but not by higher order SBP-SAT schemes. Extensive numerical experiments do indicate that also higher-order accurate SBP-SAT schemes converge with rate $p_b + 1$, however. A useful rule of thumb supported by many experiments is that, for PDE including order q derivatives in space, SBP-SAT discretizations converge with rate $\min(p_b + q, p_i)$. It has been suggested that this rate can be guaranteed for pointwise stable schemes [38], but recent work indicates that there may be exceptions [41]. To avoid further discussions on convergence rates, we will in this thesis assume that the convergence rate is the rule-of-thumb rate $\min(p_b + q, p_i)$, which usually is the case in practice.

3.3.2 Diagonal-norm SBP operators

Diagonal-norm SBP operators come with many benefits, which have made them the most commonly used ones in applications. Only diagonal H can guarantee stability for problems with variable coefficients or complex domains (see Chapter 5). Furthermore, recent efforts towards nonlinear stability show that diagonal-norm SBP operators can be used to develop entropy-consistent and entropy-stable schemes for nonlinear conservation laws [13, 14]. Diagonal H also leads to fully explicit schemes when combined with explicit time-integrators, since the inverse of a diagonal matrix is immediately available. A significant drawback, however, is that the boundary stencils are restricted to order p (see e.g. [36]), i.e. half the order of the interior stencil, which limits the convergence rate to order $p+1$ for first order equations. For example, the operator presented in Figure 3.1 is fourth-order accurate in the interior and second-order accurate in the boundary stencils, which would yield third order convergence. The corresponding norm matrix is

$$H = h \begin{bmatrix} \frac{17}{48} & & & & & & & \\ & \frac{59}{48} & & & & & & \\ & & \frac{43}{48} & & & & & \\ & & & \frac{49}{48} & & & & \\ & & & & 1 & & & \\ & & & & & 1 & & \\ & & & & & & \ddots & \end{bmatrix}.$$

Notice that the interior rows in D_1 correspond to the standard fourth-order accurate finite difference approximation:

$$(D_1\mathbf{u})_i = \frac{\frac{1}{12}u_{i-2} - \frac{2}{3}u_{i-1} + \frac{2}{3}u_{i+1} - \frac{1}{12}u_{i+2}}{h}.$$

3.3.3 Block-norm SBP operators

One can allow the norm matrix to have non-zero entries not only on the diagonal, but also in $n \times n$ blocks in the upper left and bottom right corners. This approach introduces more free parameters in the boundary closure and makes it possible to improve the boundary accuracy from p to $2p-1$ (see e.g. [36]), which yields the optimal convergence rate of order $2p$, i.e. the same order as the interior stencil. Hence, for large p the block-norm operators produce significantly more accurate results than their diagonal-norm counterparts. The

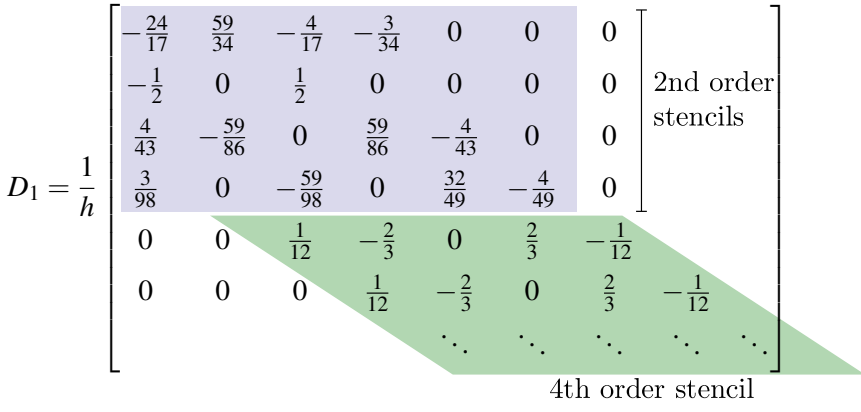

Figure 3.1. A diagonal-norm SBP operator D_1 with a fourth order interior stencil. The skewed difference stencils in the boundary block are second order accurate.

schemes are still fully explicit since H^{-1} has the same structure as H and can be computed once and for all. The drawback of block-norm operators is that they are not provably stable on curvilinear grids or for problems with variable coefficients. Deriving an energy estimate for such equations requires that H commutes with a diagonal matrix A (A typically contains the restriction of a variable coefficient to the grid on the diagonal), which can only be guaranteed for general A if H is diagonal. This lack of a stability proof reduces the usefulness of block-norm operators in realistic applications.

3.3.4 Diagonal-norm SBP operators on non-equidistant grids

If we require H to be diagonal, we may still introduce more free parameters in the boundary closure by allowing the grid points close to the boundary to be non-equidistant, see Paper II. The free parameters are tuned to minimize the leading order truncation errors of the differential operators. Here, both the locations of the grid points and the coefficients of the differential operator are outputs of the optimization process. While it remains impossible to improve the formal order of accuracy of the boundary closure beyond order p, it is possible to decrease the leading order error constants significantly. Thus the expected convergence rate as $h \to 0$ is still only $p+1$, but in the pre-asymptotic regime one often observes significantly higher rates. The optimized operators retain the provable stability of equidistant diagonal-norm operators. Numerical studies have indicated that the stability constraint on the time-step is only slightly affected by the small grid-spacings close to the boundaries.

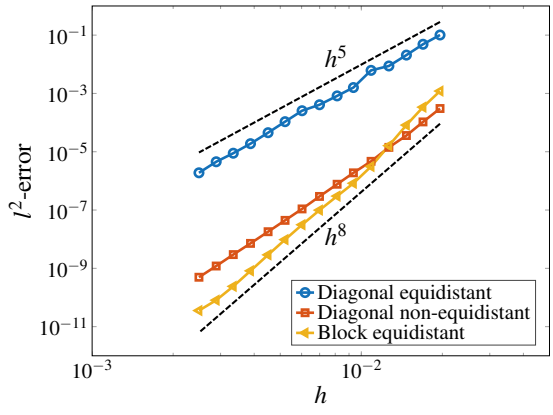

Figure 3.2. An accuracy comparison with three different SBP operators that have the same eighth order stencil in the interior.

3.3.5 Numerical experiment with different operators

To compare the accuracy properties of the different kinds of SBP operators, we consider the model problem

$$\begin{aligned} u_t + u_x &= F(x,t), \quad x \in (0,1), \quad t > 0, \\ u(0,t) &= g(t), \qquad\qquad\quad t > 0, \end{aligned}$$

where F, g, and the initial data are chosen such that the exact solution is $u(x,t) = (\cos(kx) + \sin(kx))\sin(\omega t)$ with $k = 16\pi$ and $\omega = 2\pi$. For this comparison we pick three different SBP operators with eighth order interior accuracy:

1. A traditional diagonal-norm operator on an equidistant grid
2. A traditional block-norm operator on an equidistant grid
3. The diagonal-norm operator on a non-equidistant grid from Paper II.

Note that the three schemes differ only in a few grid points close to the boundaries. We expect 1) to converge as h^5 and 2) to converge as h^8. In the limit $h \to 0$ we expect 3) to converge as h^5, but numerical experiments in double precision usually show higher rates until round-off errors start to dominate. Figure 3.2 shows the l^2-errors as functions of h. We observe the expected convergence rates for 1) and 2), and as expected 2) is much more accurate than 1) already on relatively coarse grids. By comparing 1) and 3), we can conclude that the gain in accuracy obtained by allowing a few non-equidistant grid points is enormous. We also note that 3) is on par with 2) which in the author's opinion means that there is little reason to use block-norm operators, considering the many favorable properties of diagonal norms.

4. Multi-dimensional domains

Motivated by the fact that quantum mechanical problems can be high-dimensional, we will outline how to use the SBP-SAT technique for multi-dimensional problems. Due to the curse of dimensionality, high-dimensional problems are computationally costly—for standard techniques, the storage requirements and number of floating point operations grow exponentially with the number of dimensions. Adaptive mesh refinement as in [31] can lead to significant savings, but problems with more than five or six dimensions are usually out of reach without some kind of model reduction.

Consider the advection equation in the m-dimensional cube $\Omega = [0, L]^m$,

$$\begin{aligned} u_t + \vec{a} \cdot \nabla u = 0, &\quad \vec{x} \in \Omega, &\quad t > 0\,, \\ u(\vec{x}, t) = g(\vec{x}, t), &\quad \vec{x} \in \partial\Omega_0, &\quad t > 0\,, \end{aligned} \tag{4.1}$$

where the velocity vector $\vec{a} = (a_1, a_2, \ldots, a_m)$ is assumed to be real and constant and $\vec{x} = (x_1, x_2, \ldots, x_m)$ is the position vector. Without restriction, we also assume that $\vec{a}$ has only positive components. Let Γ_i^l denote the part of $\partial\Omega$ corresponding to $x_i = 0$ and Γ_i^r the part corresponding to $x_i = L$. The second equation in (4.1) imposes a boundary condition on $\partial\Omega_0 = \bigcup_{i=1}^m \Gamma_i^l$, which corresponds to the inflow boundaries of Ω.

4.1 Multi-dimensional integration-by-parts formulas

Let $v, w \in L^2(\Omega)$ be smooth complex-valued functions and let $(\cdot, \cdot)$ and $\|\cdot\|$ denote the standard inner product and norm on $L^2(\Omega)$. Expressed in terms of the inner product, the integration-by-parts formula in multiple dimensions reads

$$\left(v, \frac{\partial w}{\partial x_i}\right) = \int_{\partial\Omega} v^* w n_i \,\mathrm{d}S - \left(\frac{\partial v}{\partial x_i}, w\right) = \int_{\Gamma_i^r} v^* w \,\mathrm{d}S - \int_{\Gamma_i^l} v^* w \,\mathrm{d}S - \left(\frac{\partial v}{\partial x_i}, w\right),$$

where n_i denotes the i:th component of $\hat{n}$, the outward unit normal. We define the Hermitian, positive semi-definite bilinear forms

$$\langle v, w \rangle_{i,l} = \int_{\Gamma_i^l} v^* w \,\mathrm{d}S\,, \quad \langle v, w \rangle_{i,r} = \int_{\Gamma_i^r} v^* w \,\mathrm{d}S\,, \tag{4.2}$$

so that the integration-by-parts formula can be written

$$\left(v, \frac{\partial w}{\partial x_i}\right) = \langle v, w\rangle_{i,r} - \langle v, w\rangle_{i,l} - \left(\frac{\partial v}{\partial x_i}, w\right). \tag{4.3}$$

The forms defined in (4.2) induce semi-norms

$$|||v|||_{i,l}^2 = \langle v, v\rangle_{i,l}, \quad |||v|||_{i,r}^2 = \langle v, v\rangle_{i,r}. \tag{4.4}$$

Using (4.3), we can derive

$$\begin{aligned}(v, \vec{a}\cdot\nabla w) &= \left(v, a_i \frac{\partial w}{\partial x_i}\right) = \langle v, a_i w\rangle_{i,r} - \langle v, a_i w\rangle_{i,l} - \left(\frac{\partial v}{\partial x_i}, a_i w\right) \\ &= \langle v, a_i w\rangle_{i,r} - \langle v, a_i w\rangle_{i,l} - (\vec{a}\cdot\nabla v, w)\end{aligned} \tag{4.5}$$

where we have adopted the Einstein summation convention to sum over repeated indices. This convention will be used henceforth. In the special case $v = w$, the formula (4.5) reduces to

$$(v, \vec{a}\cdot\nabla v) + (\vec{a}\cdot\nabla v, v) = \langle v, a_i v\rangle_{i,r} - \langle v, a_i v\rangle_{i,l} = a_i |||v|||_{i,r}^2 - a_i |||v|||_{i,l}^2. \tag{4.6}$$

4.2 Energy analysis for the continuous equation

To derive an energy estimate we multiply the PDE (4.1) by u^* and integrate in space, which yields

$$(u, u_t) = -(u, \vec{a}\cdot\nabla u). \tag{4.7}$$

Adding (4.7) and its conjugate transpose leads to

$$(u, u_t) + (u_t, u) = -(u, \vec{a}\cdot\nabla u) - (\vec{a}\cdot\nabla u, u) = -a_i |||u|||_{i,r}^2 + a_i |||u|||_{i,l}^2,$$

where we used the formula (4.6). Using the boundary condition, we obtain the energy estimate

$$\frac{\mathrm{d}}{\mathrm{d}t}\|u(\cdot,t)\|^2 = -a_i |||u|||_{i,r}^2 + a_i |||g|||_{i,l}^2,$$

which for $g = 0$ simplifies to

$$\frac{\mathrm{d}}{\mathrm{d}t}\|u(\cdot,t)\|^2 = -a_i |||u|||_{i,r}^2 \leq 0.$$

4.3 Multi-dimensional summation-by-parts operators

We introduce a tensor-product grid in Ω with N_i grid points in coordinate direction i, which leads to a total of $\mathscr{N} = N_1 N_2 \cdots N_m$ grid points. To each

coordinate direction we can associate a one-dimensional SBP operator corresponding to N_i grid points,

$$D_{x_i}^{(1\mathrm{D})} = H_{x_i}^{-1}\left(Q_{x_i} + \frac{1}{2}\left(\mathbf{e}_{x_i,r}\mathbf{e}_{x_i,r}^T - \mathbf{e}_{x_i,l}\mathbf{e}_{x_i,l}^T\right)\right) = H_{x_i}^{-1}\left(Q_{x_i} + \frac{1}{2}B_{x_i}\right).$$

In the following we will frequently use the Kronecker product. If B is an $m \times n$ matrix and C is a $p \times q$ matrix, then the Kronecker product $B \otimes C$ is the $mp \times nq$ block matrix

$$B \otimes C = \begin{bmatrix} b_{11}C & \cdots & b_{1n}C \\ \vdots & \ddots & \vdots \\ b_{m1}C & \cdots & b_{mn}C \end{bmatrix}.$$

For convenience we also introduce the notation

$$(B_1, B_2, \ldots, B_m) \cdot (C_1, C_2, \ldots, C_m) = B_i C_i,$$

for matrices B_i, C_i. We further let I_{x_i} denote the $N_i \times N_i$ identity matrix. Using the one-dimensional operators as building blocks, we can can construct multidimensional differentiation matrices:

$$D_{x_i} = I_{x_m} \otimes I_{x_{m-1}} \otimes \cdots \otimes I_{x_{i+1}} \otimes D_{x_i}^{(1\mathrm{D})} \otimes I_{x_{i-1}} \otimes \cdots \otimes I_{x_1},$$

a matrix that integrates over Ω:

$$H = H_{x_m} \otimes H_{x_{m-1}} \otimes \cdots \otimes H_{x_1},$$

matrices that integrate over the boundaries of Ω:

$$H_{\Gamma_i^l} = H_{x_m} \otimes H_{x_{m-1}} \otimes \cdots \otimes H_{x_{i+1}} \otimes \mathbf{e}_{x_i,l}\mathbf{e}_{x_i,l}^T \otimes H_{x_{i-1}} \otimes \cdots \otimes H_{x_1},$$
$$H_{\Gamma_i^r} = H_{x_m} \otimes H_{x_{m-1}} \otimes \cdots \otimes H_{x_{i+1}} \otimes \mathbf{e}_{x_i,r}\mathbf{e}_{x_i,r}^T \otimes H_{x_{i-1}} \otimes \cdots \otimes H_{x_1},$$

matrices that integrate in one coordinate direction:

$$H_i = I_{x_m} \otimes I_{x_{m-1}} \otimes \cdots I_{x_{i+1}} \otimes H_{x_i} \otimes I_{x_{i-1}} \otimes \cdots \otimes I_{x_1},$$

and matrices that select the unknowns corresponding to a certain part of $\partial\Omega$:

$$e_{\Gamma_i^l}^T = I_{x_m} \otimes I_{x_{m-1}} \otimes \cdots \otimes I_{x_{i+1}} \otimes \mathbf{e}_{x_i,l}^T \otimes I_{x_{i-1}} \otimes \cdots \otimes I_{x_1},$$
$$e_{\Gamma_i^r}^T = I_{x_m} \otimes I_{x_{m-1}} \otimes \cdots \otimes I_{x_{i+1}} \otimes \mathbf{e}_{x_i,r}^T \otimes I_{x_{i-1}} \otimes \cdots \otimes I_{x_1}.$$

Let $\mathbf{v}, \mathbf{w} \in \mathbb{C}^{\mathcal{N}}$. The matrix H induces an inner product and norm

$$(\mathbf{v}, \mathbf{w})_H = \mathbf{v}^* H \mathbf{w}, \quad \|\mathbf{v}\|_H^2 = (\mathbf{v}, \mathbf{v})_H.$$

The matrices $H_{\Gamma_i^l}$ and $H_{\Gamma_i^r}$ induce Hermitian, positive semi-definite bilinear forms

$$\langle \mathbf{v}, \mathbf{w} \rangle_{H,i,l} = \mathbf{v}^* H_{\Gamma_i^l} \mathbf{w}, \quad \langle \mathbf{v}, \mathbf{w} \rangle_{H,i,r} = \mathbf{v}^* H_{\Gamma_i^r} \mathbf{w}, \tag{4.8}$$

with corresponding semi-norms

$$|||\mathbf{v}|||_{H,i,l}^2 = \langle \mathbf{v}, \mathbf{v} \rangle_{H,i,l}, \quad |||\mathbf{v}|||_{H,i,r}^2 = \langle \mathbf{v}, \mathbf{v} \rangle_{H,i,r}. \tag{4.9}$$

The definitions (4.8) and (4.9) are analogous to (4.2) and (4.4). Moreover, D_{x_i}, which approximates $\frac{\partial}{\partial x_i}$, satisfies

$$\begin{aligned} HD_{x_i} &= H_{x_m} \otimes \cdots \otimes H_{x_{i+1}} \otimes \left(H_{x_i} D_{x_i}^{(1\mathrm{D})} \right) \otimes H_{x_{i-1}} \otimes \cdots \otimes H_{x_1} \\ &= H_{x_m} \otimes \cdots \otimes H_{x_{i+1}} \otimes \left(B_{x_i} - \left(D_{x_i}^{(1\mathrm{D})} \right)^T H_{x_i} \right) \otimes H_{x_{i-1}} \otimes \cdots \otimes H_{x_1} \\ &= H_{\Gamma_i^r} - H_{\Gamma_i^l} - D_{x_i}^T H. \end{aligned}$$

Thus, we say that D_{x_i} is an SBP operator, because it mimics the multi-dimensional integration-by-parts formula (4.3),

$$(\mathbf{v}, D_{x_i} \mathbf{w})_H = \langle \mathbf{v}, \mathbf{w} \rangle_{H,i,r} - \langle \mathbf{v}, \mathbf{w} \rangle_{H,i,l} - (D_{x_i} \mathbf{v}, \mathbf{w})_H. \tag{4.10}$$

Using the D_{x_i} operators as building blocks, we can construct an SBP operator for the gradient. We approximate

$$\nabla = \left(\frac{\partial}{\partial x_1}, \frac{\partial}{\partial x_2}, \cdots, \frac{\partial}{\partial x_m} \right),$$

by

$$\nabla_H = (D_{x_1}, D_{x_2}, \ldots, D_{x_m}).$$

Now let A_i denote diagonal matrices with a_i on the diagonal and let $\vec{A} = (A_1, \ldots, A_m)$. It follows from (4.10) that ∇_H satisfies

$$\begin{aligned} (\mathbf{v}, \vec{A} \cdot \nabla_H \mathbf{w})_H &= \mathbf{v}^* H A_i D_{x_i} \mathbf{w} = (A_i \mathbf{v})^* H D_{x_i} \mathbf{w} = (A_i \mathbf{v}, D_{x_i} \mathbf{w})_H \\ &= \langle A_i \mathbf{v}, \mathbf{w} \rangle_{H,i,r} - \langle A_i \mathbf{v}, \mathbf{w} \rangle_{H,i,l} - (D_{x_i} A_i \mathbf{v}, \mathbf{w})_H \\ &= \langle \mathbf{v}, A_i \mathbf{w} \rangle_{H,i,r} - \langle \mathbf{v}, A_i \mathbf{w} \rangle_{H,i,l} - \left(\vec{A} \cdot \nabla_H \mathbf{v}, \mathbf{w} \right)_H. \end{aligned}$$

Since ∇_H mimics the integration-by-parts property (4.5), we say that it is an SBP operator for ∇. In the special case $\mathbf{v} = \mathbf{w}$, we obtain

$$(\mathbf{v}, \vec{A} \cdot \nabla_H \mathbf{v})_H + (\vec{A} \cdot \nabla_H \mathbf{v}, \mathbf{v})_H = a_i |||\mathbf{v}|||_{H,i,r}^2 - a_i |||\mathbf{v}|||_{H,i,l}^2, \tag{4.11}$$

which mimics the formula (4.6).

4.4 Energy analysis for the semi-discrete equation

Let $\mathbf{u} \in \mathbb{C}^{\mathcal{N}}$ denote the semi-discrete solution vector and let $\mathbf{g} \in \mathbb{C}^{\mathcal{N}}$ denote a vector containing the boundary data. The SBP-SAT discretization of (4.1) reads

$$\frac{\mathrm{d}\mathbf{u}}{\mathrm{d}t} + \vec{A} \cdot \nabla_H \mathbf{u} = \tau_i \left(e_{\Gamma_i^l}^T \mathbf{u} - e_{\Gamma_i^l}^T \mathbf{g} \right), \tag{4.12}$$

where the penalty parameters τ_i are yet to be determined. Multiplying (4.12) by $\mathbf{u}^* H$ leads to

$$\left(\mathbf{u}, \frac{\mathrm{d}\mathbf{u}}{\mathrm{d}t}\right)_H = -(\mathbf{u}, \vec{A}\cdot\nabla_H\mathbf{u})_H + \mathbf{u}^* H \tau_i \left(e_{\Gamma_i^l}^T \mathbf{u} - e_{\Gamma_i^l}^T \mathbf{g}\right).$$

We consider the homogeneous case $\mathbf{g} = 0$ and make the Ansatz $\tau_i = \sigma_i H_i^{-1} e_{\Gamma_i^l}$, with σ_i being real scalars, which yields

$$\begin{aligned}\left(\mathbf{u}, \frac{\mathrm{d}\mathbf{u}}{\mathrm{d}t}\right)_H &= -(\mathbf{u}, \vec{A}\cdot\nabla_H\mathbf{u})_H + \sigma_i \mathbf{u}^* H H_i^{-1} e_{\Gamma_i^l}\left(e_{\Gamma_i^l}^T \mathbf{u}\right) \\ &= -(\mathbf{u}, \vec{A}\cdot\nabla_H\mathbf{u})_H + \sigma_i \mathbf{u}^* H_{\Gamma_i^l}\mathbf{u} \\ &= -(\mathbf{u}, \vec{A}\cdot\nabla_H\mathbf{u})_H + \sigma_i |||\mathbf{u}|||_{H,i,l}^2 .\end{aligned} \tag{4.13}$$

Adding (4.13) and its conjugate transpose leads to

$$\left(\mathbf{u}, \frac{\mathrm{d}\mathbf{u}}{\mathrm{d}t}\right)_H + \left(\frac{\mathrm{d}\mathbf{u}}{\mathrm{d}t}, \mathbf{u}\right)_H = -(\mathbf{u}, \vec{A}\cdot\nabla_H\mathbf{u})_H - (\vec{A}\cdot\nabla_H\mathbf{u}, \mathbf{u})_H + 2\sigma_i |||\mathbf{u}|||_{H,i,l}^2 .$$

Using the formula (4.11) we obtain

$$\begin{aligned}\frac{\mathrm{d}}{\mathrm{d}t}\|\mathbf{u}\|_H^2 &= -a_i |||\mathbf{u}|||_{H,i,r}^2 + a_i |||\mathbf{u}|||_{H,i,l}^2 + 2\sigma_i |||\mathbf{u}|||_{H,i,l}^2 \\ &= -a_i |||\mathbf{u}|||_{H,i,r}^2 + (a_i + 2\sigma_i) |||\mathbf{u}|||_{H,i,l}^2 .\end{aligned}$$

Choosing $\sigma_i \leq -\frac{a_i}{2}$ yields the estimate

$$\frac{\mathrm{d}}{\mathrm{d}t}\|\mathbf{u}\|_H^2 \leq 0,$$

which proves that the scheme is stable.

5. Complex geometries

To cope with non-rectangular geometries one typically uses coordinate transformations to solve a modified PDE on a rectangular domain, see Figure 5.1. To illustrate the technique, we consider the two-dimensional advection equation:

$$u_t + au_x + bu_y = 0\,, \quad (x,y) \in \Omega, \quad t > 0\,. \tag{5.1}$$

Assume that there exists a smooth one-to-one mapping

$$\begin{cases} x = x(\xi,\eta) \\ y = y(\xi,\eta) \end{cases}$$

from the unit square $\Omega' = [0,1] \times [0,1]$ to Ω. The Jacobian J of the mapping is

$$J = x_\xi y_\eta - x_\eta y_\xi\,.$$

By the chain rule,

$$\begin{bmatrix} \frac{\partial}{\partial \xi} \\ \frac{\partial}{\partial \eta} \end{bmatrix} = \begin{bmatrix} x_\xi & y_\xi \\ x_\eta & y_\eta \end{bmatrix} \begin{bmatrix} \frac{\partial}{\partial x} \\ \frac{\partial}{\partial y} \end{bmatrix}\,. \tag{5.2}$$

Because the mapping is one-to-one, it can be inverted and the Jacobian is everywhere non-zero. Inverting (5.2) yields

$$\begin{bmatrix} \frac{\partial}{\partial x} \\ \frac{\partial}{\partial y} \end{bmatrix} = \frac{1}{J} \begin{bmatrix} y_\eta & -y_\xi \\ -x_\eta & x_\xi \end{bmatrix} \begin{bmatrix} \frac{\partial}{\partial \xi} \\ \frac{\partial}{\partial \eta} \end{bmatrix}\,,$$

which allows us to rewrite (5.1) as

$$Ju_t + \alpha u_\xi + \beta u_\eta = 0\,, \quad (\xi,\eta) \in \Omega', \quad t > 0\,, \tag{5.3}$$

where

$$\alpha = (ay_\eta - bx_\eta)\,, \quad \beta = \left(bx_\xi - ay_\xi\right)\,.$$

In transforming the PDE to the reference domain Ω', we introduced variable coefficients. Hence, when dealing with non-trivial geometries we will need to handle variable coefficients, even if the coefficients a and b in the original equation are constant. We stress that diagonal-norm SBP operators are provably stable for (5.3), whereas the block-norm operators are not.

For more complex domains that cannot be smoothly mapped to the unit square, one may employ a multi-block approach where the domain is divided into blocks that are smooth mappings of the unit square. The blocks are then

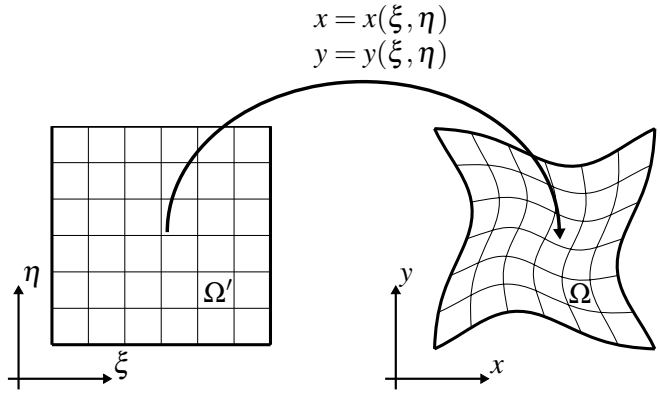

Figure 5.1. Coordinate transformation. The physical domain Ω is mapped to the reference domain Ω'.

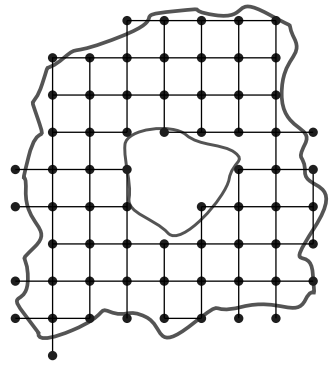

Figure 5.2. An embedded boundary grid in a complex 2D domain.

glued together with appropriate interface treatment. Ideally, the mappings should be such that the grid cell size does not vary too much—unless local mesh refinement is desired—and the cells are not too skewed. Simple and moderately complex domains are routinely gridded with high-quality multi-block curvilinear grids, but for truly complex geometries it is often too time-consuming or even impossible to generate a good grid. In such cases, finite element and finite volume methods, which support unstructured meshes, offer more flexibility than standard finite difference methods. An alternative approach is to embed the complex geometry in a Cartesian grid, see Figure 5.2, which renders the grid generation trivial. Embedded (or immersed) boundary methods have been extensively studied, but unfortunately it has proven very difficult to construct provably stable high-order methods for wave propagation problems. There are several efforts considering hyperbolic problems that are worth mentioning. In a series of papers [24, 25, 23, 22] by Kreiss et al., a second-order accurate embedded boundary method for the wave equa-

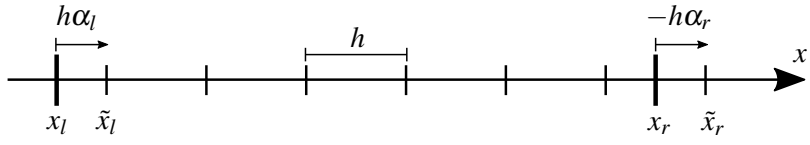

Figure 5.3. An embedded boundary grid in one dimension.

tion on second order form is developed. The method is not provably stable and requires artificial dissipation to suppress instabilities, but can handle both Dirichlet and Neumann boundary conditions as well as discontinuous wave speeds. Another successful approach for the second order wave equation is presented in [4], where a fourth-order method is achieved by using implicit difference approximations (i.e. a non-diagonal norm matrix). Again, artificial dissipation is required to suppress instabilities. An exceptional, provably stable and second order accurate method is presented in [2]. However, the technique appears to be tailored specifically to Dirichlet boundary conditions and it is not clear how to extend the approach to achieve higher-order accuracy.

In Paper III we develop a third-order accurate embedded boundary method for first-order hyperbolic systems of equations, which applies to a wide range of boundary conditions. The method is not provably stable in multiple dimensions, but extensive numerical experiments show that it is stable in practice. The method is based on embedded boundary SBP operators, which lead to provably stable embedded boundary schemes in one dimension.

5.1 Embedded boundary SBP operators

Consider the problem

$$\begin{aligned} &u_t + u_x = 0, \quad x \in (x_l, x_r), \quad t > 0, \\ &u(x_l, t) = g(t), \qquad\qquad\quad t > 0. \end{aligned} \tag{5.4}$$

As illustrated in Figure 5.3, we introduce an equidistant grid $\mathbf{x} = [x_1, x_2, \ldots, x_N]^T$, whose end points need not coincide with the interval boundaries,

$$x_i = \tilde{x}_l + (i-1)h, \quad h = \frac{\tilde{x}_r - \tilde{x}_l}{N-1}, \quad \tilde{x}_l = x_l + h\alpha_l, \quad \tilde{x}_r = x_r - h\alpha_r.$$

To discretize the equation on such a grid, we introduce an SBP operator which is a generalization of Definition 1.

Definition 3. A matrix $D_1^{\vec{\alpha}}$ is an *embedded* SBP operator for the first derivative if it can be decomposed as

$$D_1^{\vec{\alpha}} = H_{\vec{\alpha}}^{-1}\left(Q_{\vec{\alpha}} + \frac{1}{2}\mathbf{e}_r^{\vec{\alpha}}\left(\mathbf{e}_r^{\vec{\alpha}}\right)^T - \frac{1}{2}\mathbf{e}_l^{\vec{\alpha}}\left(\mathbf{e}_l^{\vec{\alpha}}\right)^T\right),$$

where $H_{\vec{\alpha}} = H_{\vec{\alpha}}^T > 0$, $Q_{\vec{\alpha}} + Q_{\vec{\alpha}}^T = 0$, and $\mathbf{e}_{l,r}^{\vec{\alpha}}$ are extrapolation operators such that for smooth functions $f \in L^2[x_l, x_r]$

$$\left(\mathbf{e}_l^{\vec{\alpha}}\right)^T \mathbf{f} \approx f(x_l), \quad \left(\mathbf{e}_r^{\vec{\alpha}}\right)^T \mathbf{f} \approx f(x_r).$$

Note that the vector $\vec{\alpha} = (\alpha_l, \alpha_r)$ contains the distances from the left and right grid boundary points to the corresponding physical boundaries. In Paper III we present diagonal-norm embedded SBP operators of orders 2, 4, and 6. The operators are parameterized by the boundary distances $\alpha_{l,r}$ and are presented on closed form for $\alpha_l, \alpha_r \in \left[-\frac{1}{2}, \frac{1}{2}\right)$.

Similar to the scheme (3.7), the embedded boundary discretization of (5.4) reads

$$\frac{\mathrm{d}\mathbf{u}}{\mathrm{d}t} + D_1^{\vec{\alpha}}\mathbf{u} = \sigma H_{\vec{\alpha}}^{-1}\mathbf{e}_l^{\vec{\alpha}}\left(\left(\mathbf{e}_l^{\vec{\alpha}}\right)^T \mathbf{u} - g\right).$$

With $g = 0$, the discrete energy method leads to

$$\frac{\mathrm{d}}{\mathrm{d}t}\|\mathbf{u}\|_{H_{\vec{\alpha}}}^2 = -\left|\left(\mathbf{e}_r^{\vec{\alpha}}\right)^T \mathbf{u}\right|^2 + (1+2\sigma)\left|\left(\mathbf{e}_l^{\vec{\alpha}}\right)^T \mathbf{u}\right|^2,$$

which shows that the embedded boundary scheme is stable for $\sigma \leq -\frac{1}{2}$.

6. Summary of papers

6.1 Paper I

When the norm matrix H is required to be diagonal, the accuracy of the SBP operator D_1 of order $2p$ in the interior is reduced to order p in a few grid points close to the boundaries. For first order hyperbolic equations, this typically limits the global convergence rate to order $p+1$. If one allows H to be block-diagonal, the boundary accuracy can be improved to $2p-1$, which yields the optimal convergence rate of order $2p$. Hence, from an accuracy perspective, block-norm operators appear superior to their diagonal counterparts. Unfortunately, when deriving energy estimates, H can only be permitted to be non-diagonal if the PDE has constant coefficients and is discretized on a Cartesian grid. Thus, in case of variable coefficients or curvilinear grids, block-norm operators are not provably stable, which significantly limits their usefulness for realistic problems.

To obtain high accuracy while maintaining stability, we set out to stabilize the block-norm operators. We identify that the instabilities are caused by the boundary stencils, and therefore construct artificial dissipation that targets only the boundary points. The dissipation is constructed to damp high-frequency modes efficiently without decreasing the order of accuracy. Numerical experiments show that the artificial dissipation can indeed be tuned to stabilize the scheme without decreasing accuracy or significantly increasing stiffness.

Contributions
The author of this thesis performed the numerical experiments in 2D and wrote parts of the manuscript.

6.2 Paper II

We address the same problem as in Paper I, i.e. the low boundary accuracy of diagonal-norm operators, but with a different approach. Instead of stabilizing block-norm operators, we focus on improving the accuracy of diagonal-norm operators. By allowing a non-equidistant grid close to the boundaries, we introduce more free parameters in the construction of the operators. The free parameters are tuned to minimize the leading order truncation errors of the difference operators. Here, both the locations of the grid points and the coefficients of the difference operator are outputs of the optimization process. While

it remains impossible to improve the formal order of accuracy of the boundary to closure beyond order p, it is possible to decrease the leading order error constants significantly. Numerical experiments demonstrate the superiority of the novel operators, when compared to compared to traditional operators on an equidistant grid. As the new operators come with a diagonal norm matrix, they admit energy estimates just like their traditional counterparts, and are thus provably stable.

Contributions
The author of this thesis extended the proposed method to curvilinear grids, performed the numerical experiments in 2D, and wrote parts of the manuscript.

6.3 Paper III

The possibly largest drawback of high-order finite difference methods is their inflexibility when dealing with complex geometries. While multi-block curvilinear grids do a good job in moderately complicated domains, they may be very cumbersome or even impossible to generate in truly complex geometries. Immersing or embedding complicated boundaries in Cartesian background grids is a long-standing research topic that has gained a lot of attention. By not requiring the grid to conform with the boundaries, the grid generation process is rendered trivial. However, stable high-order embedded boundary methods for wave propagation problems have proven inherently difficult to construct.

We derive provably stable embedded boundary methods in one spatial dimension. By essentially applying the 1D method on each grid line, we extend the method to 2D. The method applies to general first-order hyperbolic systems of equations with well-posed boundary conditions. However, in the extension from 1D to 2D the provable stability is lost. We find that artificial dissipation is required to stabilize the 2D method. Extensive numerical experiments show that it is possible to devise artificial dissipation that stabilizes the scheme, preserves third order global accuracy, and yet combines well with explicit time-stepping.

Contributions
The work was performed in close collaboration between the authors. The author of this thesis focused on the extension to 2D.

6.4 Paper IV

Sound propagation problems are commonly solved using simplified models. Examples include ray-tracing [33] and so-called parabolic equation (PE) [40]

methods. They are usually fast, but not always accurate. We consider a benchmark problem proposed in [32], involving a sound source in nontrivial axisymmetric geometry, where the objective is to compute the sound pressure levels one meter above ground. We develop a finite difference method for the second order wave equation, which serves as a reliable model. We analyze the numerical treatment of boundary conditions in curvilinear coordinates and consider non-reflecting boundary conditions. Using the grid-converged finite difference solution of the wave equation as the true solution, we evaluate the accuracy of several different ray-tracing and PE methods.

Contributions
The author of this thesis had the main responsibility for preparing the manuscript and performed most of the computations. The ideas were developed in close collaboration with the co-authors.

6.5 Paper V

Most quantum dynamical computations are based on the SE. It is well known that the equation is not valid for high kinetic energies and that it does not describe spin dynamics. When required, such effects are often approximated by various correcting procedures. In this paper, we propose to base computations on the DE rather than corrected versions of the SE. The DE inherently accounts for relativistic effects and describes the dynamics of particle spin. Because it is a system of four equations, practitioners often consider the DE too computationally expensive compared to the SE. We argue that, due to the differences in dispersion relation illustrated in Figure 2.1, the DE is in some senses easier to solve numerically, which decreases the difference in computational cost.

We derive stable finite difference discretizations of the DE and show that, as expected, the equations give similar results for low kinetic energies. We also demonstrate that, for high energies, the (uncorrected) SE does not produce accurate results. In particular, we consider the classical problem of quantum tunneling, where the two models predict quite different outcomes. The SE predicts that particles can tunnel through potential barriers that exceed the kinetic energy, but the tunneling probability decays exponentially inside the barrier. In [21], Klein showed that for high-energy particles the DE predicts a tunneling probability that tends to a nonzero limit as the barrier height goes to infinity—this counter-intuitive phenomenon is known as Klein tunneling. Loosely speaking, the DE predicts a much larger tunneling probability than the SE, which is demonstrated by numerical experiments.

Contributions
The author of this thesis had the main responsibility for preparing the manuscript and performed all computations. The ideas were developed in consultation with the co-authors.

6.6 Paper VI

Aharonov and Bohm showed that a charged particle may acquire a phase shift by circling around a completely shielded magnetic flux [3]. This counter-intuitive effect can not be explained by classical mechanics, as the electromagnetic field vanishes at the location of the particle, which thus experiences no Lorentz force. The origin of the phase shift is topological: it does not depend on the exact shape of the particle's path around the magnetic flux. While topological phase shifts have been observed in molecular spectroscopy, direct observation of Aharonov-Bohm (AB) effects in molecular scattering have been elusive in the past. Here, we demonstrate an adiabatic AB effect by simulating the dynamics of unpolarized slow neutrons that scatter on a straight current-carrying wire. The acquired phase shift causes destructive interference in the forward direction, providing an unambiguous signature of the adiabatic AB effect. We further show that the effect remains as the neutron velocity is increased, which opens up the possibility to observe the effect in experiments with higher velocities in the adiabatic regime.

Contributions
The first author developed the ideas and prepared the manuscript in consultation with the co-authors. The author of this thesis performed all numerical experiments.

6.7 Paper VII

For partial differential equations with small geometric features in the spatial domain, locally refined meshes allow for accurate simulation without introducing too many spatial unknowns and are thus computationally efficient. In the case of wave propagation problems, one typically combines the spatial discretization with explicit time-integration. The combination of local mesh refinement and explicit time-stepping, however, is problematic—the Courant-Friedrichs-Lewy (CFL) stability restriction [8] on the time-step depends on the smallest mesh-size. If the locally refined region is small compared to the entire computational domain, using a tiny time-step everywhere is too expensive. The same usually holds for using an implicit scheme everywhere. Instead, one might hope to use different time-steps or a combination of implicit and explicit schemes. Here, we focus on explicit local time-stepping (LTS) schemes,

which are fully explicit but decrease the time-step where the small elements are located. Thus they permit a larger time-step in the coarser regions of the mesh without violating the CFL stability condition.

Grote et al. [16] derived LTS methods based on explicit Runge–Kutta (RK) methods. Their LTS methods allow for two different time steps—one global and one local—which is all that is needed when the mesh contains only one level of refinement. However, when the mesh contains nested patches of refinement, any local time-step will be unnecessarily small in some regions. To allow for an appropriate time-step at each level of mesh refinement, multi-level local time-stepping (MLTS) methods have been proposed [11]. In this paper, we start from the RK-based LTS methods by Grote et al. and derive fully explicit MLTS methods, which permit arbitrarily many different time-steps. Thus, they adapt well to all mesh configurations. The derivation applies to any explicit RK method, including e.g. low-storage methods. We prove that the MLTS-RK schemes retain the order of accuracy of the underlying RK method. Numerical experiments with the second order wave equation, discretized in space using SBP-SAT finite difference methods and continuous finite element methods, show the expected convergence rates. They also show that the MLTS methods retain the CFL condition of the underlying method at each level of refinement.

Contributions

The paper was developed in close collaboration between the authors.

7. Sammanfattning på svenska

Vågor uppträder i många former i vår omgivning: ljuden vi uppfattar är tryckvågor, jordskalven efter en jordbävning är seismiska vågor och vattenvågorna på en sjö är en typ av gravitationsvågor. Mindre påtagliga i vardagen, men ändå av stor betydelse för oss, är kvantmekaniska vågor. På atomära längdskalor kan alla partiklar bete sig som vågor och vice versa. Ljus, till exempel, visar ett vågliknande beteende när det träffar vattendroppar, splittras upp i olika färger och bildar en regnbåge. Samtidigt kan den fotoelektriska effekten, där en metall som belyses med tillräckligt kortvågigt ljus avger elektroner, bara förklaras fullständigt om ljus består av partiklar eller vågpaket (så kallade fotoner) snarare än vågor. På motsvarande sätt beter sig elektroner, neutroner och protoner ofta som vågor, även om vi gärna tänker på dem som massiva partiklar.

Vågfenomenen ovan kan alla beskrivas med partiella differentialekvationer. Den endimensionella advektionsekvationen är det enklaste exemplet på en ekvation som beskriver vågutbredning,

$$\begin{aligned} &u_t + u_x = 0\,, \quad x \in (0,L)\,, \quad t > 0\,, \\ &u(0,t) = g(t)\,, \qquad\qquad\quad t > 0\,, \end{aligned} \tag{7.1}$$

där notationen u_z betyder partiell derivata av u med avseende på z, x är en rumskoordinat, t är tid och $g(t)$ är en känd funktion. Vi antar att lösningen u är känd vid begynnelsetiden $t = 0$. Ekvationen (7.1) parallellförflyttar alla toppar och dalar i $u(x,t)$ åt höger med hastighet ett. Vid inflödet $x = 0$ behöver vi ange vad som flödar in i domänen; utan randvillkoret $u(0,t) = g(t)$ skulle lösningen inte vara unik.

Ekvationen (7.1) är visserligen så enkel att den kan lösas med papper och penna, men i allmänhet är partiella differentialekvationer så komplicerade att de är mycket svåra eller till och med omöjliga att lösa exakt. I sådana fall kan vi lösa dem approximativt genom att programmera numeriska metoder i datorer. Den här avhandlingen behandlar *effektiva* numeriska metoder. För att förklara vilka egenskaper en effektiv metod bör ha använder vi (7.1) som exempel. Det finns många olika metoder, men alla innefattar att på något sätt representera lösningen u med ett ändligt antal värden. Ett sätt att diskretisera den rumsliga delen av (7.1) är att införa beräkningsnätet

$$x_j = (j-1)h, \quad j = 1,\ldots,N\,,$$

där $h = \frac{L}{N-1}$. Vi kan sedan bilda en diskret lösningsvektor $\mathbf{u} = [u_1, u_2, \ldots, u_N]^T$, så att $u_i(t)$ approximerar $u(x_i, t)$. Om vi exempelvis approximerar rumsderivatan med finita differenser får vi ett system av N ordinära differentialekvationer,

$$\frac{\mathrm{d}\mathbf{u}}{\mathrm{d}t} = M\mathbf{u} + \mathbf{G}(t)\,. \tag{7.2}$$

Exakt hur matrisen M och den vektorvärda funktionen $\mathbf{G}(t)$ ser ut beror på vilken metod som används. Ekvationen är semi-diskret i den mening att vi har diskretiserat rummet men låtit tiden förbli kontinuerlig. För att lösa det ursprungliga problemet (7.1) måste vi så småningom även diskretisera tiden i (7.2), men här fokuserar vi på rumsdelen.

Genom att använda en numerisk metod på (7.1) har vi gått från en partiell differentialekvation till ett system av N ordinära differentialekvationer. Fördelen är att de ordinära ekvationerna rent konceptuellt är enklare än de partiella, men en nackdel är att vi nu står inför N ekvationer istället för en, där N kan vara ett stort tal. Hur man än beter sig för att lösa (7.2) kommer det krävas många aritmetiska operationer, vilket gör det till en jobbig uppgift för en människa. Som tur är fungerar datorer annorlunda än vi – de är väldigt bra på att göra enkla saker snabbt. Moderna datorer kan utan problem utföra miljarder aritmetiska operationer per sekund. Genom att implementera numeriska algoritmer i datorer har vi möjlighet att simulera vågfenomen som beskrivs av betydligt mer komplicerade ekvationer än (7.1).

När man använder numeriska metoder gäller det dock att vara försiktig. Även för den till synes enkla advektionsekvationen finns det mycket som kan gå fel. Instabila metoder, till exempel, kommer göra att den numeriska lösningen växer exponentiellt med tiden, trots att den sanna lösningen inte växer alls. För att undvika sådana bakslag vill vi använda *robusta* metoder, som ger rimliga resultat under många olika omständigheter. Allra helst vill vi kunna garantera att den numeriska lösningen konvergerar mot den sanna lösningen när h går mot noll. Nackdelen med att minska h är förstås att N samtidigt ökar, vilket gör algoritmen mer beräkningskrävande så att simuleringen kommer ta längre tid. För att kunna lösa riktigt stora problem vill vi därför använda *billiga* metoder. Med billig menar vi här att det, när allt går bra, krävs relativt lite datorkraft för att beräkna lösningen till en angiven noggrannhet.

Utöver datorresurser bör vi tänka på hur många arbetstimmar vi människor behöver lägga ner. En önskvärd egenskap är naturligtvis att metoden är *enkel* på så sätt att den är lätt att programmera, men det är inte allt. När man undersöker vågfenomen vet man till en början oftast inte exakt vilket problem man vill simulera. Kanske vill man kunna variera några parametrar, lägga till termer till ekvationerna, eller byta randvillkor. Om den numeriska metoden är alltför skräddarsydd till ett enskilt problem kan vi bli tvungna att helt byta metod, vilket leder till mycket extra arbete. Vi vill därför helst använda *flexibla* metoder, som med bara små ändringar kan ta hand om ett brett spektrum av problem.

Baserat på ovanstående diskussion drar vi slutsatsen att effektiva numeriska metoder bör vara robusta, billiga, enkla och flexibla. För partiella differentialekvationer finns det väldigt många olika metoder som alla har sina styrkor och svagheter. Exempel på populära metoder är finit volyms-, finita element-, finit differens- och spektralmetoder. I den här avhandlingen behandlar vi enbart finit differens-metoder. De är lätta att förstå och enkla att implementera. När det kommer till vågutbredningsproblem bör metoder ha hög noggrannhetsordning för att vara billiga [27]. Jämfört med finit volyms- och finita element-metoder har finit differens-metoder fördelen att de kan ha hög ordning och samtidigt lämpa sig för fullt explicit tidsstegning. Tyvärr blir differensmetoderna i regel mindre robusta när man ökar ordningen, speciellt när man måste ta hänsyn till randvillkor. Förr gjorde detta att man ofta tvingades välja mellan billiga och robusta metoder. Idag har så kallade SBP-SAT-metoder [10, 39] löst det problemet genom att erbjuda ett systematiskt tillvägagångssätt för att konstruera robusta metoder av hög ordning. Tekniken är också flexibel i den mening att den fungerar för många olika ekvationer med olika typer av randvillkor.

Den här avhandlingen kan delas in i tre olika delar. I den första delen fokuserar vi på att förbättra existerande SBP-SAT-metoder. I Manuskript I och II tar vi fram metoder med högre noggrannhet än standardmetoderna. I Manuskript III konstruerar vi en metod för inbäddade ränder, som gör det enklare att hantera ekvationer inom komplicerade domäner. Avhandlingens andra del visar hur SBP-SAT-metoden kan tillämpas på vågutbredningsproblem inom akustik (Manuskript IV) och kvantmekanik (Manuskript V och VI). I den tredje delen utvecklar vi i Manuskript VII en effektiv, fullt explicit tidsstegningsmetod som lämpar sig för lokalt förfinade beräkningsnät.

Acknowledgements

First of all, I would like to express my sincerest gratitude to my adviser Ken Mattsson. Ken, together with Kristoffer Virta you made me want to become a PhD student by showing me how much fun it can be to do research. Since then you have guided me through the scientific world and, perhaps more importantly, provided an endless supply of inspiration, enthusiasm and optimism. Thanks also to my coadviser Tomas Edvinsson for sharing your knowledge, for always being friendly, and for all the nice lunches we have had, discussing research, movies, and life. I am also grateful to my collaborators Mark Carpenter, Ilkka Karasalo, Michaela Mehlin, and Erik Sjöqvist for being so very friendly and willing to share their expertise.

Further, I consider myself privileged to have met so many nice people at TDB. Many of you have become good friends of mine, but there are some that I would like to give special mention to. I can not imagine what the last two years would have been like without my protégé, mentor, office mate, and friend, Jonatan Werpers. I am also grateful to Fredrik Hellman, Hanna Holmgren, and Simon Sticko, for being the wonderful people that they are and for supporting me whenever I needed it the most. Additionally, I would like to thank Ylva Rydin for her valuable comments on a draft of this comprehensive summary.

Sist men absolut inte minst vill jag tacka min familj: mamma, pappa och Isabelle. Utan allt ni har gjort för mig under alla år hade den här avhandlingen aldrig tryckts, skrivits eller ens påbörjats!

References

[1] S. Abarbanel, A. Ditkowski, and B. Gustafsson. On error bounds of finite difference approximations to partial differential equations—temporal behavior and rate of convergence. *Journal of Scientific Computing*, 15:79–116, 2000.

[2] S. Abarbanel, A. Ditkowski, and A. Yefet. Bounded error schemes for the wave equation on complex domains. *Journal of Scientific Computing*, 26:67–81, 2006.

[3] Y. Aharonov and D. Bohm. Significance of electromagnetic potentials in the quantum theory. *Physical Review*, 115:485–491, 1959.

[4] D. Appelö and N. A. Petersson. A fourth-order accurate embedded boundary method for the wave equation. *SIAM Journal on Scientific Computing*, 34:A2982–A3008, 2012.

[5] J. Berg and J. Nordström. Superconvergent functional output for time-dependent problems using finite differences on summation-by-parts form. *Journal of Computational Physics*, 231:6846–6860, 2012.

[6] M. H. Carpenter, D. Gottlieb, and S. Abarbanel. Time-stable boundary conditions for finite-difference schemes solving hyperbolic systems: methodology and application to high-order compact schemes. *Journal of Computational Physics*, 111:220–236, 1994.

[7] M. H. Carpenter and D. Gottlieb. Spectral methods on arbitrary grids. *Journal of Computational Physics*, 129:74–86, 1996.

[8] R. Courant, K. Friedrichs, and H. Lewy. Über die partiellen Differenzengleichungen der mathematischen Physik. *Mathematische Annalen*, 100:32–74, 1928.

[9] D. C. Del Rey Fernández, P. D. Boom, and D. Zingg. A generalized framework for nodal first derivative summation-by-parts operators. *Journal of Computational Physics*, 266:214–239, 2014.

[10] D. C. Del Rey Fernández, J. Hicken, and D. Zingg. Review of summation-by-parts operators with simultaneous approximation terms for the numerical solution of partial differential equations. *Computers & Fluids*, 95:171–196, 2014.

[11] J. Diaz and M. J. Grote. Energy conserving explicit local time stepping for second-order wave equations. *SIAM Journal on Scientific Computing*, 31:1985–2014, 2009.

[12] P. A. M. Dirac. The quantum theory of the electron. *Proceedings of the Royal Society of London A: Mathematical, Physical and Engineering Sciences*, 117:610–624, 1928.

[13] T. C. Fisher, M. H. Carpenter, J. Nordström, N. K. Yamaleev, and C. Swanson. Discretely conservative finite-difference formulations for nonlinear conservation laws in split form: Theory and boundary conditions. *Journal of Computational Physics*, 234:353–375, 2013.

[14] T. C. Fisher and M. H. Carpenter. High-order entropy stable finite difference schemes for nonlinear conservation laws: finite domains. *Journal of Computational Physics*, 252:518–557, 2013.

[15] G. J. Gassner. A skew-symmetric discontinuous Galerkin spectral element discretization and its relation to SBP-SAT finite difference schemes. *SIAM Journal on Scientific Computing*, 35:1233–1253, 2013.

[16] M. J. Grote, M. Mehlin, and T. Mitkova. Runge–Kutta-Based Explicit Local Time-Stepping Methods for Wave Propagation. *SIAM Journal on Scientific Computing*, 37:A747–A775, 2015.

[17] B. Gustafsson. The convergence rate for difference approximations to mixed initial boundary value problems. *Mathematics of Computation*, 29:396–406, 1975.

[18] B. Gustafsson, H.-O. Kreiss, and J. Oliger. *Time dependent problems and difference methods*. John Wiley & Sons, Inc., 1995.

[19] B. Gustafsson, H.-O. Kreiss, and A. Sundström. Stability theory of difference approximations for mixed initial boundary value problems. *Mathematics of Computation*, 26:649–686, 1972.

[20] J. Hicken and D. Zingg. Superconvergent functional estimates from summation-by-parts finite-difference discretizations. *SIAM Journal on Scientific Computing*, 33:893–922, 2011.

[21] O. Klein. Die Reflexion von Elektronen an einem Potentialsprung nach der relativistischen Dynamik von Dirac. *Zeitschrift für Physik*, 53:157–165, 1928.

[22] H.-O. Kreiss and N. A. Petersson. An embedded boundary method for the wave equation with discontinuous coefficients. *SIAM Journal on Scientific Computing*, 28:2054–2074, 2006.

[23] H.-O. Kreiss and N. A. Petersson. A second order accurate embedded boundary method for the wave equation with Dirichlet data. *SIAM Journal on Scientific Computing*, 27:1141–1167, 2006.

[24] H.-O. Kreiss, N. A. Petersson, and J. Yström. Difference approximations for the second order wave equation. *SIAM Journal on Numerical Analysis*, 40:1940–1967, 2002.

[25] H.-O. Kreiss, N. A. Petersson, and J. Yström. Difference approximations of the Neumann problem for the second order wave equation. *SIAM Journal on Numerical Analysis*, 42:1292–1323, 2004.

[26] H.-O. Kreiss and G. Scherer. Finite element and finite difference methods for hyperbolic partial differential equations. *Mathematical Aspects of Finite Elements in Partial Differential Equations., Academic Press, Inc.*, 1974.

[27] H.-O. Kreiss and J. Oliger. Comparison of accurate methods for the integration of hyperbolic equations. *Tellus*, 24:199–215, 1972.

[28] P. D. Lax and R. D. Richtmyer. Survey of the stability of linear finite difference equations. *Communications on Pure and Applied Mathematics*, 9:267–293, 1956.

[29] K. Mattsson. Summation by parts operators for finite difference approximations of second-derivatives with variable coefficients. *Journal of Scientific Computing*, 51:650–682, 2012.

[30] K. Mattsson. Diagonal-norm summation by parts operators for finite difference approximations of third and fourth derivatives. *Journal of Computational*

Physics, 274:432–454, 2014.

[31] A. Nissen, K. Kormann, M. Grandin, and K. Virta. Stable difference methods for block-oriented adaptive grids. *Journal of Scientific Computing*, 65:486–511, 2015.

[32] S. Parakkal, K. E. Gilbert, D. Xiao, and H. E. Bass. A generalized polar coordinate method for sound propagation over large-scale irregular terrain. *Journal of the Acoustical Society of America*, 128:2573–2580, 2010.

[33] C. L. Pekeris. Theory of propagation of explosive sound in shallow water. *Geological Society of America Memoirs*, 27:1–116, 1948.

[34] G. Scherer. *On the existence of energy estimates for difference approximations for hyperbolic systems*. Ph. D. thesis, Uppsala University, 1977.

[35] E. Schrödinger. Quantisierung als Eigenwertproblem (Vierte Mitteilung). *Annalen der Physik*, 386:109–139, 1926.

[36] B. Strand. Summation by parts for finite difference approximations for d/dx. *Journal of Computational Physics*, 110:47–67, 1994.

[37] M. Svärd and J. Nordström. Stability of finite volume approximations for the Laplacian operator on quadrilateral and triangular grids. *Applied Numerical Mathematics*, 51:101–125, 2004.

[38] M. Svärd and J. Nordström. On the order of accuracy for difference approximations of initial-boundary value problems. *Journal of Computational Physics*, 218:333–352, 2006.

[39] M. Svärd and J. Nordström. Review of summation-by-parts-operators schemes for initial-boundary-value problems. *Journal of Computational Physics*, 268:17–38, 2014.

[40] F. D. Tappert. The parabolic approximation method. *Wave Propagation and Underwater Acoustics*, edited by J. B. Keller and J. S. Papadakis, Lecture Notes in Physics, Vol. 70, 1977.

[41] S. Wang and G. Kreiss. Convergence of summation-by-parts finite difference methods for the wave equation. *Journal of Scientific Computing*, in press.

Acta Universitatis Upsaliensis

Digital Comprehensive Summaries of Uppsala Dissertations from the Faculty of Science and Technology 1463

Editor: The Dean of the Faculty of Science and Technology

A doctoral dissertation from the Faculty of Science and Technology, Uppsala University, is usually a summary of a number of papers. A few copies of the complete dissertation are kept at major Swedish research libraries, while the summary alone is distributed internationally through the series Digital Comprehensive Summaries of Uppsala Dissertations from the Faculty of Science and Technology. (Prior to January, 2005, the series was published under the title "Comprehensive Summaries of Uppsala Dissertations from the Faculty of Science and Technology".)

Distribution: publications.uu.se
urn:nbn:se:uu:diva-310124

ACTA
UNIVERSITATIS
UPSALIENSIS
UPPSALA
2017